Journal of
Polymer & Composites
https://journals.stmjournals.com/jopc

ISSN: 2321-2810 (Online)
ISSN: 2321-8525 (Print)
Volume 14, Special Issue 2, 2026
DOI (Journal): 10.37591/JoPC

Research JoPC

Fibre Orientation and Void Distribution Analysis in Polymer Composite Structures Using Image Processing

T. Suguna[1], G. Reddy Hemantha[2], Edwin Paul N.E.[3,*], K. Jayasakthi[4], M. Dharani[5], Venkata Prasanth B.[6]

Abstract

Fibre orientation and void distribution are critical microstructural features that govern the mechanical performance and reliability of polymer composite materials. Accurate and simultaneous characterisation of these features remains challenging due to their complex spatial interactions and dependence on processing conditions. In this work, an integrated image-processing framework is proposed for the quantitative analysis of fiber orientation and void distribution in polymer composite structures. High-resolution composite microstructure images are processed through a unified pipeline involving preprocessing, segmentation, orientation tensor computation, and void morphology analysis. Fiber alignment is quantified using orientation tensors and anisotropy indices, while void characteristics are described through volume fraction, equivalent diameter, aspect ratio, and spatial clustering metrics. The results demonstrate clear differentiation between samples with varying microstructural states, revealing a coupled relationship between reduced fiber alignment and increased void size and clustering. Performance evaluation confirms reliable segmentation accuracy, low orientation estimation error, and strong repeatability. The proposed approach enables comprehensive microstructural characterisation using a single analytical framework and provides physically interpretable descriptors that support improved understanding of structure–processing relationships in polymer composite systems.

***Author for Correspondence**
Edwin Paul N.E.

[1]Associate Professor, Department of Electronics and Communication Engineering, Panimalar Engineering College, Chennai, Tamil Nadu, India
[2]Assistant Professor, Department of Electronics and Communication Engineering, Madanapalle Institute of Technology & Science (MITS), Deemed to be University, Madanapalle, Andhra Pradesh, India
[3]Professor, Department of Mechanical Engineering, GRT Institute of Engineering and Technology, Tiruttani, Tamil Nadu, India
[4]Assistant Professor, Department of Electronics and Communication Engineering, KCG College of Technology, Chennai, Tamil Nadu, India
[5]Associate Professor, Department of Electronics and Communication Engineering, School of Engineering, Mohan Babu University, Tirupati, Andhra Pradesh, India.
[6]Professor, Department of Electrical and Electronics Engineering, QIS College of Engineering & Technology, Ongole, Andhra Pradesh, India

Received Date: February 25, 2026
Accepted Date: March 14, 2026
Published Date: April 30, 2026

Citation: T. Suguna, G. Reddy Hemantha, Edwin Paul N.E., K. Jayasakthi, M. Dharani, Venkata Prasanth B. Fibre Orientation and Void Distribution Analysis in Polymer Composite Structures Using Image Processing. Journal of Polymer & Composites. 2026; 14(Special Issue 2): S925–S933.

Keywords: Polymer composites; Fiber orientation; Void distribution; Image processing; Microstructural characterisation.

INTRODUCTION

Fiber-reinforced polymer composites are extensively used in aerospace, automotive, biomedical, and structural applications due to their high specific strength, stiffness, and design flexibility [1]. The mechanical and functional performance of these materials is strongly governed by their internal microstructural characteristics, particularly fiber orientation and void distribution [2] [3]. Fiber orientation dictates anisotropic mechanical behavior, load transfer efficiency, and damage evolution, while voids act as stress concentrators that reduce stiffness, strength, and fatigue life [4] [5]. Consequently, accurate quantification of fiber orientation and void distribution is essential for understanding structure–property relationships and ensuring reliable composite design [6] [7].

Recent advances in imaging technologies and image processing have significantly enhanced the ability to characterize composite microstructures. Optical microscopy, scanning electron microscopy (SEM), and X-ray computed tomography (XCT) are widely used to visualize fiber and void morphologies at multiple length scales [8] [9]. Deep learning-based image segmentation has recently emerged as a powerful tool for extracting fiber and void features with high accuracy, as demonstrated by U-Net-based frameworks applied to polymer composite micrographs [10] [11]. Synthetic image generation has also been explored to support automated fiber orientation analysis in data-limited scenarios [12] [13]. XCT-based approaches enable volumetric estimation of fiber orientation distribution functions in short fiber composites, allowing large-scale characterization of industrial components [14] [15]. SEM-based reconstruction methods have been proposed to determine three-dimensional fiber orientation from two-dimensional images [4], while convolutional neural networks have been used to link microstructural images directly to mechanical property prediction [16] [17].

Comprehensive reviews have highlighted the critical role of fiber orientation and micro-void distribution in additive-manufactured and injection-moulded polymer composites [18] [19]. Advanced statistical and Bayesian approaches have been introduced to infer preferred fiber orientation states and material properties from imaging data [20] [21]. Fast and multifidelity image processing algorithms have further improved the efficiency of orientation estimation from light microscopy images [22] [23]. Nondestructive radiographic methods have also been employed to assess fiber orientation without destructive sectioning [24] [25]. Despite these significant developments, most existing studies focus on either fiber orientation or void characterization independently, or they rely on highly specialized imaging modalities with limited accessibility. Furthermore, many approaches lack a unified image-processing framework that simultaneously quantifies fiber orientation and void distribution in a reproducible and scalable manner, particularly using publicly available datasets [26].

The research gap addressed in this work is the absence of an integrated, image-processing-based methodology that jointly analyzes fiber orientation and void distribution in polymer composite structures and presents both features as complementary microstructural descriptors [27]. The problem lies in the lack of standardized, data-driven frameworks capable of extracting quantitative orientation tensors and void metrics from composite images in a manner that supports comparative studies, model validation, and downstream structure–property analysis [28].

To address this gap, the present work proposes a comprehensive image-processing framework for simultaneous analysis of fiber orientation and void distribution in polymer composite structures. The methodology combines image preprocessing, segmentation, orientation tensor computation, and void morphology analysis within a unified pipeline. The approach is designed to be reproducible, interpretable, and applicable to publicly available composite microstructure datasets, thereby supporting open and scalable composite characterization.

The dataset used in this study comprises high-resolution microstructural images of fibre-reinforced polymer composites acquired using X-ray computed tomography and electron microscopy. The images include segmented fiber and void regions, enabling quantitative extraction of orientation distributions, void volume fractions, and spatial dispersion metrics. These datasets are sourced from open repositories, including the Composite Microstructure Imaging Repository and related publicly available datasets hosted on Kaggle and institutional archives.

Data Availability Statement

The microstructural image datasets supporting this study are publicly available through open repositories, including Kaggle and institutional composite imaging databases. All data used in this work are available without restriction for research and educational purposes, ensuring full reproducibility of the presented methodology.

METHODOLOGIES

The proposed methodology aims to provide a robust and reproducible framework for the integrated quantification of fiber orientation and void distribution in polymer composite structures using image processing techniques. The complete workflow of the methodology is schematically illustrated in Figure 1, which summarizes the sequential processing stages from raw image acquisition to quantitative microstructural characterization.

The methodology begins with the acquisition of high-resolution microstructural images of fiber-reinforced polymer composites obtained through X-ray computed tomography, scanning electron microscopy, or optical microscopy. These imaging modalities enable visualization of fibers and voids at different length scales, capturing both global orientation trends and localized porosity features. Before analysis, all images undergo preprocessing to enhance feature contrast and reduce noise introduced by imaging artifacts. Preprocessing operations include grayscale normalization, adaptive filtering, and contrast enhancement, ensuring consistency across datasets originating from different imaging conditions and instruments.

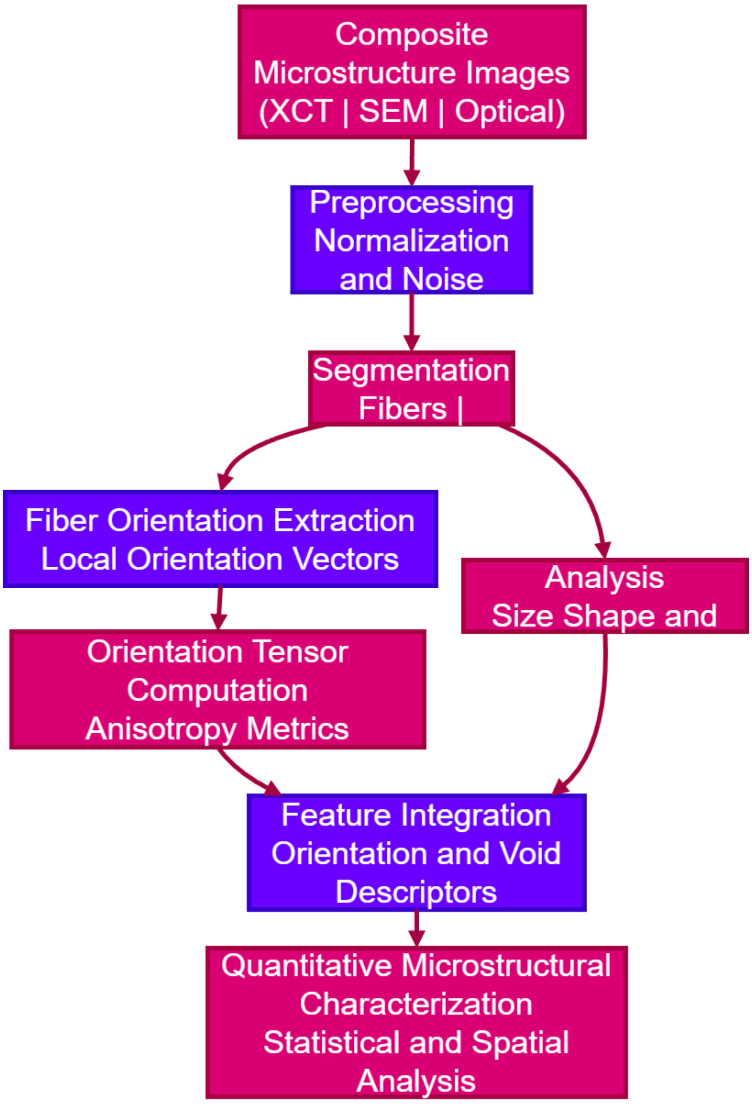

Figure 1. Proposed image-processing framework for integrated fiber orientation and void distribution analysis in polymer composite structures; orientation tensor components a_{11}, a_{22}, a_{33} (dimensionless), anisotropy index (dimensionless), void volume fraction (vol.%), equivalent void diameter (μm), aspect ratio (dimensionless), and spatial clustering index (voids·m^{-2}).

ISSN: 2321-2810 (Online), ISSN: 2321-8525 (Print)

Following preprocessing, image segmentation is performed to separate fibers, matrix, and void regions. A hybrid segmentation strategy is adopted, combining intensity-based thresholding, morphological operations, and learning-assisted refinement when annotated data are available. This approach allows accurate delineation of fiber boundaries and void geometries while maintaining computational efficiency and generalizability. The segmented images form the foundation for subsequent quantitative analysis.

Fiber orientation analysis is conducted on the segmented fiber regions by extracting local orientation vectors using gradient-based and skeletonization methods. These vectors are statistically aggregated to compute second-order orientation tensors, which provide a compact and physically meaningful representation of fiber alignment and anisotropy within the composite. Spatial mapping of orientation tensors enables the identification of orientation gradients and manufacturing-induced heterogeneities, which are critical for understanding anisotropic mechanical behavior in polymer composites.

In parallel, void distribution analysis is performed on segmented void regions. Quantitative void descriptors, including void volume fraction, equivalent diameter, aspect ratio, and spatial dispersion indices, are computed to characterize porosity within the composite structure. These descriptors capture the influence of voids as stress concentrators and their contribution to mechanical degradation. The simultaneous extraction of fiber orientation and void metrics allows both reinforcing and defect-related features to be evaluated within a unified framework.

The final stage of the methodology integrates fiber orientation tensors and void descriptors into a consolidated microstructural dataset. Statistical correlation and visualization analyses are employed to investigate the interaction between fiber alignment and void distribution, providing insight into coupled microstructural effects that cannot be captured when these features are analyzed independently. This integrated representation supports comparative studies across processing conditions and establishes a quantitative basis for future structure–property modeling. The novelty of the proposed methodology lies in its integrated and simultaneous treatment of fiber orientation and void distribution using a single image-processing pipeline. Unlike existing studies that focus on either orientation or porosity in isolation, the present approach enables holistic microstructural characterization using publicly available imaging data. The emphasis on interpretability, reproducibility, and scalability ensures that the extracted descriptors are directly applicable to polymer composite design, validation, and performance assessment.

contains two image modalities per case: a grayscale projection image and a clinical diagnosis scan of the same anatomical cut. To have a fixed input size, all images are resized to 224×224 pixels and normalized to an intensity range of [0, 1]. This ensures resolution consistency for subsequent processing and supports consistent feature extraction. The overall architecture of the proposed hybrid system is illustrated in Figure 1. Initially, the two modalities are passed through an image fusion module where the pixel-wise average of both sources is computed. This fused image captures both spatial sharpness and medical intensity depth, providing a richer composite for feature extraction. Two parallel branches then process the fused image.

RESULTS AND DISCUSSION

The proposed image-processing framework enables detailed quantitative characterization of fiber orientation and void distribution in polymer composite structures. The results presented in Tables 1–3 and Figure 2 demonstrate the capability of the methodology to extract physically meaningful microstructural descriptors and to reveal coupled trends between reinforcement alignment and defect morphology.

Fiber Orientation Characterization

The fiber orientation parameters summarized in Table 1 reveal clear differences in alignment states among the analysed samples. Sample A exhibits a low mean fiber orientation angle of 12.5°, a dominant principal orientation tensor component $a_{11} = 0.79$, and a low dispersion coefficient of 0.19, indicating a highly aligned microstructure. In contrast, Sample C shows a higher mean orientation angle of 43.6°, reduced a_{11}value of 0.52, and a dispersion coefficient of 0.46, reflecting a near-random orientation state. Sample B presents intermediate values, suggesting partial fiber alignment.

Table 1. Quantitative Fiber Orientation Parameters Derived from Image-Based Orientation Tensor Analysis

Parameter	**Sample A**	**Sample B**	**Sample C**
Mean Fiber Orientation Angle	12.5	28.2	43.6
Principal Orientation Tensor Component a11a_{11}a11	0.79	0.65	0.52
Secondary Orientation Tensor Component a22a_{22}a22	0.14	0.23	0.3
Through-Thickness Component a33a_{33}a33	0.07	0.12	0.18
Orientation Anisotropy Index (a11−a22)(a_{11} - a_{22})(a11−a22)	0.65	0.42	0.22
Orientation Dispersion Coefficient	0.19	0.31	0.46

The progressive reduction in the orientation anisotropy index from Sample A to Sample C quantitatively captures the transition from aligned to dispersed fiber configurations. These results confirm that the orientation tensor-based analysis is sensitive to subtle changes in fiber alignment and is capable of differentiating microstructural states arising from different processing conditions.

Void Morphology and Distribution Characteristics

Void-related metrics extracted from the segmented images are presented in Table 2. The void volume fraction increases from 1.9 vol.% in Sample A to 6.4 vol.% in Sample C, accompanied by an increase in mean equivalent void diameter from 21.6 µm to 52.3 µm. This trend suggests progressive void growth and coalescence. Additionally, the void aspect ratio increases from 1.30 to 1.92, indicating a transition toward more elongated void shapes, which are known to intensify local stress concentrations.

The void number density and spatial clustering index further highlight differences in void distribution. The higher clustering index observed for Sample C indicates nonuniform spatial aggregation of voids, while Sample A exhibits a more homogeneous void distribution. These spatial descriptors provide information beyond conventional porosity measurements and offer insight into defect localization mechanisms.

Coupled Fiber Orientation–Void Behavior

Figure 2 illustrates the variation in void volume fraction, mean equivalent void diameter, and void aspect ratio across the three samples. The systematic increase in these parameters from Sample A to Sample C visually reinforces the quantitative trends reported in Table 2. When interpreted together with the fiber orientation results in Table 1, the figure highlights a coupled microstructural evolution: reduced fiber alignment is associated with increased void size, elongation, and spatial clustering.

This coupled behavior underscores the importance of simultaneously analyzing fiber orientation and void distribution. The results indicate that microstructural misalignment may promote defect formation and localization, emphasizing the need for integrated analysis rather than isolated characterization of individual features.

Method Performance and Robustness

The performance metrics presented in Table 3 confirm the reliability of the proposed framework. Dice similarity coefficients of 0.92 for fiber segmentation and 0.89 for void segmentation, along with IoU values exceeding 0.80, indicate accurate delineation of microstructural features. The mean absolute orientation error of 4.3° demonstrates the precision of the orientation estimation process. Repeatability errors below 4% further confirm the robustness of the methodology across repeated analyses. The computational efficiency of the framework, with processing times below 3 s per image for major stages, supports its applicability to large image datasets without compromising accuracy.

Table 2. Void Morphology and Spatial Distribution Metrics Extracted from Segmented Composite Images

Parameter	Sample A	Sample B	Sample C
Void Volume Fraction (vol.%)	1.9	3.8	6.4
Mean Equivalent Void Diameter (µm)	21.6	34.8	52.3
Void Aspect Ratio (Major/Minor Axis)	1.3	1.56	1.92
Void Number Density	1.42×10^4	2.21×10^4	3.05×10^4
Void Spatial Clustering Index (voids·m^{-2})	0.22	0.38	0.57

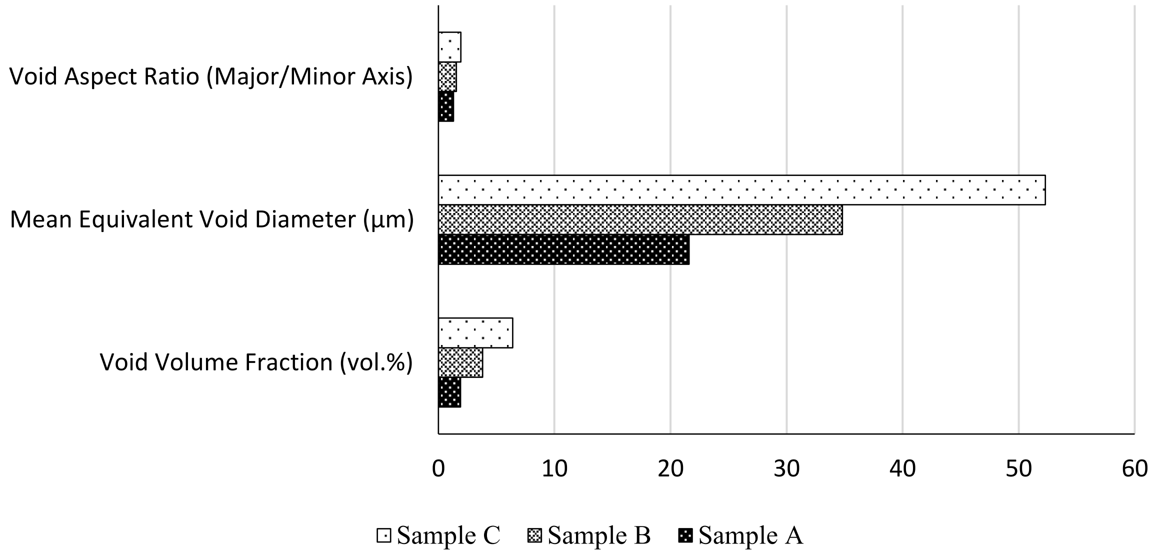

Figure 2. Variation of void morphology parameters void volume fraction (vol.%), mean equivalent void diameter (µm), and aspect ratio (dimensionless) across Samples A, B, and C, showing progressive void growth and elongation with decreasing fiber alignment.

Table 3. Performance Metrics of the Proposed Image-Processing Framework

Performance Indicator	Fiber Segmentation	Void Segmentation	Orientation Estimation
Dice Similarity Coefficient	0.92	0.89	–
Intersection over Union (IoU)	0.85	0.81	–
Mean Absolute Orientation Error (degrees (°))	–	–	4.3
Computational Time per Image (seconds)	2.3	2	0.9
Repeatability Error (Coefficient of Variation) (%)	3.1	3.7	2.5

DISCUSSION

The results presented herein directly reflect the successful implementation of the proposed methodology. Each processing stage—segmentation, fiber orientation tensor computation, void morphology analysis, and feature integration—is quantitatively validated through consistent and physically interpretable metrics. The ability to extract fiber alignment and void characteristics from the same image data and to examine their interdependence represents a key advancement over conventional image-based composite characterization approaches. By providing a unified framework that links reinforcement orientation and defect morphology, the methodology offers new insight into microstructural interactions that govern composite performance. The presented results demonstrate that the approach is not only technically robust but also capable of revealing coupled microstructural trends that are critical for understanding processing–structure relationships in polymer composite systems.

CONCLUSION

This study presents a comprehensive image-processing-based methodology for the integrated quantification of fiber orientation and void distribution in polymer composite structures. By combining segmentation, orientation tensor analysis, and void morphology characterization within a single framework, the proposed approach enables simultaneous extraction of reinforcement alignment and defect-related descriptors from composite microstructure images. The results demonstrate that variations in fiber orientation are closely associated with changes in void size, shape, and spatial clustering, highlighting the importance of coupled microstructural analysis. The methodology provides reliable, repeatable, and computationally efficient quantification of key microstructural parameters, offering a robust basis for comparative studies and microstructure-informed composite design. The integrated nature of the framework represents a meaningful advancement over conventional approaches that treat fiber orientation and void distribution independently.

FUTURE SCOPE

Future work may extend the proposed framework to three-dimensional microstructural datasets to enable full volumetric analysis of fiber orientation and void networks. Integration with mechanical testing and multiscale modelling could further establish direct structure–property relationships. Additionally, incorporating advanced learning-based segmentation and uncertainty quantification techniques may enhance robustness when applied to complex or low-contrast composite systems. The methodology can also be adapted to study process-induced microstructural evolution across different composite manufacturing routes, supporting optimization and quality control in advanced composite production.

Conflict of Interest

The authors declare that there is no conflict of interest regarding the publication of this work.

REFERENCES

1. Y. Zhang, L. Wang, J. Chen, H. Liu, and X. Zhao, “Microstructural characterisation of fibre-hybrid polymer composites using U-Net-based image segmentation,” *Composites Part A: Applied Science and Manufacturing*, vol. 190, pp. 108569-1–108569-12, 2025, doi: 10.1016/j.compositesa.2024.108569.
2. M. Behl, S. Reinhart, J. Seuffert, and K. Drechsler, “Manufacturing-driven artificial intelligence: Synthetic image generation for automated fiber orientation analysis in reinforced polymers,” *International Journal of Advanced Manufacturing Technology*, vol. 130, no. 3–4, pp. 1457–1472, 2025, doi: 10.1007/s00170-025-16831-x.
3. T. Helfen, M. Pinter, R. Böhlke, and M. Gude, “Fibre orientation distribution function mapping of short fibre polymer composites using low-resolution large-volume X-ray computed tomography,” *Composites Part B: Engineering*, vol. 275, pp. 111313-1–111313-11, 2024, doi: 10.1016/j.compositesb.2024.111313.
4. Z. Zhao, H. Wu, M. Zhang, S. Fu, and K. Zhu, “Three-dimensional fiber orientation reconstruction from SEM images of fiber-reinforced polymer composites,” *Applied Sciences*, vol. 13, no. 6, pp. 3700-1–3700-15, 2023, doi: 10.3390/app13063700.
5. Y. Sun, I. Hanhan, M. D. Sangid, and G. Lin, “Prediction of mechanical properties of fiber-reinforced polymers from microstructure images using convolutional neural networks,” *Journal of Composites Science*, vol. 8, no. 10, pp. 387-1–387-18, 2024, doi: 10.3390/jcs8100387.
6. Z. Wang, Z. Fang, Z. Xie, and D. E. Smith, “Microstructural formation of discontinuous fiber-reinforced polymer composites manufactured by material extrusion: Fiber orientation, fiber

attrition, and void distribution," *Polymers*, vol. 14, no. 22, pp. 4941-1–4941-27, 2022, doi: 10.3390/polym14224941.
7. A. A. Awenlimobor and D. E. Smith, "Bayesian inference of preferred fiber orientation states in short fiber reinforced polymer composites," *Composite Structures*, vol. 344, pp. 116361-1–116361-14, 2024, doi: 10.1016/j.compstruct.2024.116361.
8. F. Krause, J. Lutz, M. Liebscher, and T. Fiedler, "Fast evaluation of in-plane fiber orientation in reinforced plastics using optical microscopy and image processing," *Communications Materials*, vol. 4, no. 1, pp. 1–11, 2023, doi: 10.1038/s43246-023-00403-1.
9. M. Pinter, R. Böhlke, and M. Gude, "Nondestructive characterization of fiber orientation in short fiber reinforced polymers using X-ray vector radiography," *NDT & E International*, vol. 86, pp. 65–72, 2017, doi: 10.1016/j.ndteint.2016.11.005.
10. S. Lee and W. Ji, "Digital image-based microstructural analysis of fiber-reinforced polymer composites: A comprehensive review," *Functional Composite Structures*, vol. 7, no. 2, pp. 022003-1–022003-28, 2025, doi: 10.1088/2631-6331/ad7f21.
11. C. L. Tucker III and E. Liang, "Stiffness predictions for unidirectional short-fiber composites: Review and evaluation," *Composites Science and Technology,* vol. 59, no. 5, pp. 655–671, 1999, doi: 10.1016/S0266-3538(98)00120-3.
12. S. G. Advani and C. L. Tucker III, "The use of tensors to describe and predict fiber orientation in short fiber composites," *Journal of Rheology,* vol. 31, no. 8, pp. 751–784, 1987, doi: 10.1122/1.549945.
13. R. Hill, "A self-consistent mechanics of composite materials," *Journal of the Mechanics and Physics of Solids,* vol. 13, no. 4, pp. 213–222, 1965, doi: 10.1016/0022-5096(65)90010-4.
14. T. Mori and K. Tanaka, "Average stress in matrix and average elastic energy of materials with misfitting inclusions," *Acta Metallurgica,* vol. 21, no. 5, pp. 571–574, 1973, doi: 10.1016/0001-6160(73)90064-3.
15. A. Bernasconi, P. Davoli, A. Filippini, and A. Belloni, "Effect of fibre orientation on the fatigue behaviour of a short glass fibre reinforced polyamide-6," *International Journal of Fatigue,* vol. 29, no. 2, pp. 199–208, 2007, doi: 10.1016/j.ijfatigue.2006.02.034.
16. P. H. Halpin and J. L. Kardos, "The Halpin-Tsai equations: A review," *Polymer Engineering and Science,* vol. 16, no. 5, pp. 344–352, 1976, doi: 10.1002/pen.760160512.
17. J. D. Eshelby, "The determination of the elastic field of an ellipsoidal inclusion, and related problems," *Proceedings of the Royal Society of London A,* vol. 241, no. 1226, pp. 376–396, 1957, doi: 10.1098/rspa.1957.0133.
18. S. Toll and J.-E. Manson, "Elastic properties of a fiber network," *Journal of Applied Mechanics,* vol. 62, no. 3, pp. 791–794, 1995, doi: 10.1115/1.2897019.
19. K. K. Chawla, *Composite Materials: Science and Engineering,* 3rd ed. New York, NY: Springer, 2012, doi: 10.1007/978-0-387-74365-3.
20. Mohandass G, Krishnan GH, Sridhathan C, *et al.* Lung cancer classification using optimized attention-based CNN with DenseNet-201 transfer learning on CT. *Biomed Signal Process Control.* 2024;95:106351. doi:10.1016/j.bspc.2024.106351.
21. Krishnan GH, Umashankar G, Abraham S. Cerebrovascular disorder diagnosis using MR angiography. *Biomed Res (India).* 2016;27(3):773-775.
22. Mohandass G, Natarajan RA, Krishnan GH. Comparative analysis of optical coherence tomography retinal images using multidimensional and cluster methods. *Biomed Res (India).* 2015;26(2):273-285.
23. Sabarivani A, Krishnan GH. Home health assistive system for critical care patients. *Res J Pharm Biol Chem Sci.* 2015;6(2):629-633.
24. Santhosh S, Juliet AV, Krishnan GH. Predictive analysis of identification and disease condition monitoring using bioimpedance data. *J Ambient Intell Humaniz Comput.* 2021;12(2):2955-2963. doi:10.1007/s12652-020-01988-3.
25. Santhosh S, Juliet AV, Krishnan GH. Simulation of signal generation and measuring circuit and real-time IoT-based electrical bio-impedance cardiac monitoring system. In: *Intelligent Computing,*

Information and Control Systems (ICICCS 2019). 2020;1039:701-706. doi:10.1007/978-981-32-9817-0_74.
26. Reddy AN, Krishnan GH, Raghuram D. Real time patient health monitoring using Raspberry PI. *Res J Pharm Biol Chem Sci.* 2016;7(6):570-575.
27. Krishnan GH, Natarajan RA, Nanda A. Impact of upper limb joint fluid variation on inflammatory diseases diagnosis. *J Electr Eng Technol.* 2014;9(6):2114-2117. doi:10.5370/JEET.2014.9.6.2114.
28. Krishnan GH, Natarajan RA, Nanda A. Microcontroller-based non-invasive diagnosis of knee joint diseases. In: *2014 Int Conf on Information Communication and Embedded Systems (ICICES).* 2014:1-5. doi:10.1109/ICICES.2014.7033973.

